Hot Topics from BABAR

BaBar Collaboration

Hot topics from BABAR

Vasia Shelkov
BaBar Collaboration
Lawrence Berkeley National Laboratory
Berkeley, USA

1 Introduction

We present preliminary results of searches for B mesons decaying into the charmless final states, using around 50 fb^{-1} of data collected at the $\Upsilon(4S)$ resonance with the *BABAR* detector at the SLAC PEP-II asymmetric B Factory. We describe measurements with the BaBar data of the branching fractions for B decays to charmless quasi-two-body final states containing η' mesons. We find $\mathcal{B}(B^+ \to \eta' K^+) = (67 \pm 5 \pm 5) \times 10^{-6}$, $\mathcal{B}(B^0 \to \eta' K^0) = (46 \pm 6 \pm 4) \times 10^{-6}$, and $\mathcal{B}(B^0 \to \eta' K^{*0}) = (4.0^{+3.5}_{-2.4} \pm 1.0) \times 10^{-6}$ ($< (13.3) \times 10^{-6}$). We also measure the branching fractions $\mathcal{B}(B^\pm \to K^\pm \pi^\mp \pi^\pm) = (59.2 \pm 4.7 \pm 4.9) \times 10^{-6}$ and $\mathcal{B}(B^\pm \to K^\pm K^\mp K^\pm) = (34.7 \pm 2.0 \pm 1.8) \times 10^{-6}$, and provide the 90% confidence upper limits $\mathcal{B}(B^\pm \to \pi^\pm \pi^\mp \pi^\pm) < 15 \times 10^{-6}$ and $\mathcal{B}(B^\pm \to K^\pm K^\mp \pi^\pm) < 7 \times 10^{-6}$.

2 Charmless B meson decays to $\eta' K$ or $\eta' K^{*0}$

In this note, we report results of searches for B decays to three charmless quasi-two-body final states involving η' mesons. We include the decay modes $B^+ \to \eta' K^+$, $B^0 \to \eta' K^0$ and $B^0 \to \eta' K^{*0}$. These data contain an on-peak integrated luminosity of $56.4(52.0)\ fb^{-1}$ for the $B \to \eta' K (B^0 \to \eta' K^{*0})$ analyses. In addition there is $6.4\ fb^{-1}$ of off-peak exposure. The full on-peak sample corresponds to $(61.6 \pm 0.7) \times 10^6$ $B\overline{B}$ pairs. A B meson candidate is characterized kinematically by the difference in energy $\Delta E = (E_0 E_B - \boldsymbol{p_0} \cdot \boldsymbol{p_B} - \frac{1}{2}s)/\sqrt{s}$, and beam energy constrained mass $m_{EC} = \sqrt{E_B^{*2} - p_B^{*2}}$. Backgrounds arise primarily from combinatorics among light quark pair events from the continuum under the $\Upsilon(4S)$. Decays from genuine B mesons predominantly produce charmed, hence heavier daughters that are kinematically distinct from the charmless modes we seek. We extract the signal yields with a maximum likelihood fit to sets of weakly correlated observables. Each of the PDFs typically involves several parameters that are determined with various samples of data and Monte Carlo and are fixed for the ML fit. The input variables used in the fits are ΔE, M_{ES}, the invariant mass of the resonance R candidate (m_R), the Fisher

discriminant ($\mathcal{F}$), and, where relevant, the the helicity angle of the ρ ($\mathcal{H}$). The PDF determination for the likelihood fit is accomplished with use of signal Monte Carlo for the signal decays, and sideband data for the continuum background. Peaking distributions (signal masses, ΔE, $\mathcal{F}$) are parameterized

Table 1: Final ML fit results.

Quantity	$\eta'_{\eta\pi\pi}K^+$	$\eta'_{\rho\gamma}K^+$	$\eta'_{\eta\pi\pi}K^0$	$\eta'_{\rho\gamma}K^0$	$\eta'_{\eta\pi\pi}K^{*0}$	
					Run 1	Run 2
Events to fit						
On-resonance	2199	34492	665	7400	656	1074
Off-resonance	254	3847	59	790	92	138
Signal yield						
On-res data	152^{+14}_{-13}	293^{+23}_{-22}	29^{+7}_{-6}	106^{+14}_{-13}	$0.0^{+1.3}_{-0.0}$	$5.2^{+3.9}_{-2.8}$
Off-res data	$-1.6^{+1.8}_{-0.9}$	$-1.3^{+4.0}_{-2.9}$	$0.0^{+0.7}_{-0.0}$	$0.0^{+2.8}_{-0.0}$	$0.0^{+0.5}_{-0.0}$	$0.0^{+0.6}_{-0.0}$
Combinations/event	1.18	1.08	1.18	1.07	1.15	1.10
$B\overline{B}$ BG subtraction	0	13 ± 6	0	4.1 ± 2.1	0.7 ± 1.4	0.9 ± 1.1
MC ϵ (%)	23.1	24.0	23.5	24.5	16.9	16.9
ML-fit ϵ/bias (%)	99.0	94.4	100.0	97.0	105.9	105.3
Trk/Neut/PID corr. (%)	96.1	96.2	102.1	102.2	96.8	96.8
$\prod \mathcal{B}_i$ (%)	17.4	29.5	6.0	10.1	11.5	11.5
Corr. $\epsilon \times \prod \mathcal{B}_i$ (%)	3.82	6.42	1.43	2.46	1.99	1.98
Stat. sign. (σ)	26	20	10	15	0	1.9
$\mathcal{B}(\times 10^{-6})$	65 ± 6	71 ± 6	32 ± 7	67 ± 9	$0^{+2.2}_{-0.0}$	$7.9^{+5.8}_{-4.2}$
UL (stat. only)	−	−	−	−	8.7	17
UL (incl. syst.)	−	−	−	−	12	24

Table 1 shows the results for off-peak and on-peak data. The statistical error on the number of events is taken as the change in the central value when the quantity $\chi^2 \equiv -2\ln\mathcal{L}$ changes by one unit. The statistical significance is taken as the square root of the difference between the value of χ^2 for zero signal and the value at its minimum. We illustrate the best fit likelihood function by projection of the yields and PDFs in m_{ES} and ΔE, with cuts to emphasize the signal-like events. It can be found in Figure 1. We are left with about a three standard deviation discrepancy between our measurements of $B^0 \to \eta'K^0$ in the two η' decay modes. We include in the following section the cross checks we have performed to rule out unaccounted systematics that could affect either result. Finding no evidence of inconsistency within either mesurement, we present the weighted average for this as well as the charged mode as our final measurements of the neutral and charged
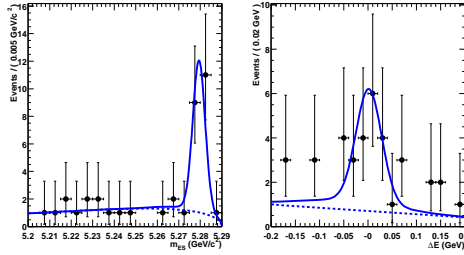
Figure 1: Projection of the on-resonance data and PDF projected onto (left) m_{ES} and (right) ΔE, for $B^0 \to \eta' \, (\eta' \to \eta \pi^+ \pi^-) K^0$.

$B \to \eta' K$ branching fractions. For modes where the central value is not significant, we include systematics in the 90% CL upper limit. This approach amounts to folding systematics in quadrature into the likelihood function before integrating to obtain the 90% CL. We have found significant event yields in five of the decay chains studied here, as reported in Table 1. Where we have multiple chains for a given mode we combine the results, representing the uncorrelated errors by distributions in $\chi^2 = -2 \log \frac{\mathcal{L}}{\mathcal{L}_{\max}}$ which are added. Where the significance is less than four standard deviations, we quote also (Bayesian) 90% C.L. upper limits, defined by the solution B to the condition $\int_0^B \mathcal{L}(b) db / \int_0^\infty \mathcal{L}(b) db = 0.9$. The final results are: $\mathcal{B}(B^+ \to \eta' K^+) = (67 \pm 5 \pm 5) \times 10^{-6}$, $\mathcal{B}(B^0 \to \eta' K^0) = (46 \pm 6 \pm 4) \times 10^{-6}$, $\mathcal{B}(B^0 \to \eta' K^{*0}) = (4.0^{+3.5}_{-2.4} \pm 1.0) \times 10^{-6}$ ($< (13.3) \times 10^{-6}$). They are generally in agreement with those previously reported, with smaller errors (more restrictive limit). In particular we confirm the rather larger than predicted [2] rate for $B \to \eta' K$ obtained by the CLEO Collaboration [3]. Conjectured sources of η' enhancement include flavor singlet [4], charm enhanced [8], and constructively interfering internal penguin diagrams [2, 5].

3 Measurements of the branching fractions of charmless three-body charged B decays

We present updated preliminary results on the branching fractions of charged charmless three-body $B^\pm \to h^\pm h^\mp h^\pm$ decays, where $h = \pi$ or K, with no assumptions about intermediate resonances and with open charm contributions subtracted. Charge conjugate initial and final states are assumed throughout this document, unless stated otherwise. The data sample consists of 56.2 million $B\overline{B}$ pairs, corresponding to an integrated luminosity of 51.5 fb^{-1} collected at the $\Upsilon(4S)$ resonance (on-resonance) during the 2000-2001 run. Charged particles are identified by the Cherenkov angle θ_c

and the number of photons measured with the DIRC. The typical separation between pions and kaons varies from $> 8~\sigma$ at 2.0GeV/c to 2.5σ at 4.0GeV/c, where σ is the average resolution on θ_c. The kaon selection efficiency is approximately 80%, which is the product of the particle identification algorithm efficiency with geometrical acceptance, for a pion mis-identification probability of 2%. The total branching fraction for each $B^\pm \to h^\pm h^\mp h^\pm$ mode is measured over the whole Dalitz plot - all resonant and non-resonant contributions are included. A set of selection criteria is applied to reconstruct each mode separately. Each Dalitz plot is divided into many equal area cells to enable us to find the selection efficiency as a function of position in the Dalitz plot. We also take into account continuum backgrounds and cross-feed between each signal mode from K and π mis-identification. We use dE/dx information from the SVT and DCH, and the Cherenkov angle and number of photons measured by the DIRC for tracks with momenta above 700 MeV/c, to identify charged pions and kaons. Since we are only interested in charmless decays, we need to veto candidates that contain charm mesons. We remove B candidates when the invariant mass of the combination of any two of its daughter tracks (of opposite charge) is within 3 σ of the mass of D^0, J/ψ or $\psi(2S)$ mesons. Here, σ is 10.0 MeV/c^2 for D^0 and 15.0 MeV/c^2 for J/ψ and $\psi(2S)$. All possible kaon and pion combinations are tested for the D^0 veto, while only the K^+K^- and $\pi^+\pi^-$ hypotheses are tested for the J/ψ and $\psi(2S)$ vetoes, since the background from these decays is from leptonic decays, in which the leptons have been mis-identified as pions or kaons. The electron veto helps to reduce the combinatorial background from J/ψ and $\psi(2S)$ decays that would otherwise pass the 3 σ invariant mass veto. We reduce tlight quark and charm continuum backgrounds by imposing requirements on two topological event shape variables computed in the $\Upsilon(4S)$ rest frame: the cosine of the angle θ_T and Fisher discriminant [6]. The residual background level is estimated from the observed number of events in a sideband region, located near to the signal region in the m_{ES}- ΔE plane, and then extrapolating into the signal region by using a multiplicative factor, R. We define R to be the ratio of the number of background candidates in the signal region to the number in the sideband region. As mentioned previously, the branching fractions for each signal mode are measured over the whole Dalitz plot, and each Dalitz plot is divided up into many cells so that the bin-by-bin variation of the selection efficiency can be found for each plot. The signal region is defined to be $|m_{ES} - m_B| < 8.0$ MeV/c^2 and $|\Delta E - \langle \Delta E \rangle| < 60.0$ MeV, where $\langle \Delta E \rangle$ is the mean value of ΔE for on-resonance data for the calibration sample $B^- \to D^0 \pi^-$, $D^0 \to K^- \pi^+$, and m_B is the nominal mass of the charged B meson [7]. The GSB region is defined to be $5.21 < m_{ES} < 5.25$ GeV/c^2 and $|\Delta E - \langle \Delta E \rangle| < 100.0$ MeV. The Dalitz plot for each signal mode is divided into cells with equal area 1.0 GeV^4, and large samples of Monte Carlo signal events are used to obtain the signal and cross-feed selection efficiencies across each Dalitz plot. Table 2 shows the signal and cross-feed selection efficiencies for the modes, averaged over the Dalitz plots. The uncertainties on the signal efficiencies and cross-feed prob-

Table 2: Efficiencies and cross-contamination probabilities between the signal modes derived from Monte Carlo samples. For example, the probability that an event $K^\pm\pi^\mp\pi^\pm$ will be reconstructed as $\pi^\pm\pi^\mp\pi^\pm$ is $(1.7 \pm 0.1) \times 10^{-2}$.

Selected as	Input Decay Mode			
	$\pi^\pm\pi^\mp\pi^\pm$	$K^\pm\pi^\mp\pi^\pm$	$K^\pm K^\mp\pi^\pm$	$K^\pm K^\mp K^\pm$
$\pi^\pm\pi^\mp\pi^\pm$	$(15.3 \pm 0.2) \times 10^{-2}$	$(1.7 \pm 0.1) \times 10^{-2}$	$(1.4 \pm 0.9) \times 10^{-4}$	$(1.1 \pm 3.2) \times 10^{-5}$
$K^\pm\pi^\mp\pi^\pm$	$(3.6 \pm 0.4) \times 10^{-3}$	$(15.1 \pm 0.2) \times 10^{-2}$	$(3.2 \pm 0.2) \times 10^{-2}$	$(4.0 \pm 1.7) \times 10^{-4}$
$K^\pm K^\mp\pi^\pm$	$(0.0 \pm 0.2) \times 10^{-3}$	$(2.9 \pm 0.4) \times 10^{-3}$	$(17.7 \pm 0.3) \times 10^{-2}$	$(5.5 \pm 0.2) \times 10^{-2}$
$K^\pm K^\mp K^\pm$	$(0.0 \pm 0.2) \times 10^{-3}$	$(0.0 \pm 0.2) \times 10^{-3}$	$(1.7 \pm 0.2) \times 10^{-3}$	$(21.6 \pm 0.3) \times 10^{-2}$

abilities are the combination of statistical errors on the number of events selected in the Monte Carlo samples relative to the total number generated, as well as systematic uncertainties arising from the difference between Monte Carlo simulation and on-resonance data. The fractional uncertainties for the Dalitz plot variation for the cross-feed probabilities ($\Delta\epsilon_i''/\epsilon_i''$) are approximately 30%. Finally, there is a systematic uncertainty on the overall normalisation, $N_{B\overline{B}}$, which is obtained from a dedicated study to find the number of B mesons produced in the data sample. This is found to have a systematic uncertainty of 1.5%. Figures 2 to 5 show the ΔE and m_{ES} distributions for the signal region for each of the modes. Each plot shows the expected levels continuum and $B\overline{B}$ background (solid and dashed lines, respectively). Figures 6 to 9 show the unbinned Dalitz plots for the signal modes in the GSB and signal regions, where no efficiency corrections have been applied. Only the upper half of the symmetrical Dalitz plot is shown for the $B^\pm \to \pi^\pm\pi^\mp\pi^\pm$ and $B^\pm \to K^\pm K^\mp K^\pm$ channels, where the x and y axes show the minimum and maximum values of the Dalitz plot variables, respectively. There are clear signals for the modes $B^\pm \to K^\pm\pi^\mp\pi^\pm$ and $B^\pm \to K^\pm K^\mp K^\pm$. No signal is observed for $B^\pm \to K^\pm K^\mp\pi^\pm$, and the result for $B^\pm \to \pi^\pm\pi^\mp\pi^\pm$ is interpreted as an upper limit on the branching fraction, although there is a positive excess of signal events with 2.2 σ significance. Since there are a large number of events in the selected samples, we can assume that the number of signal and background events observed in the signal region are Gaussian distributed. The 90% C.L. upper limits are computed using the standard prescription for a one-sided confidence interval from a Gaussian distributed measurement.
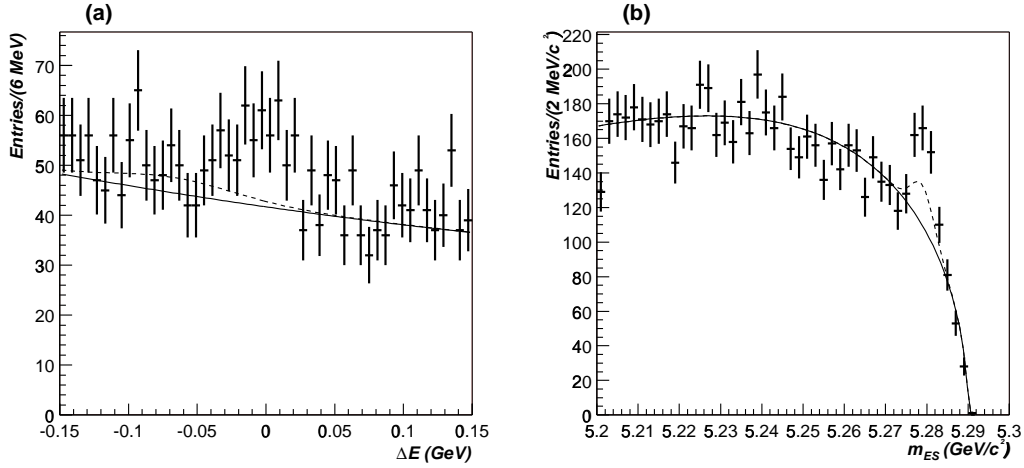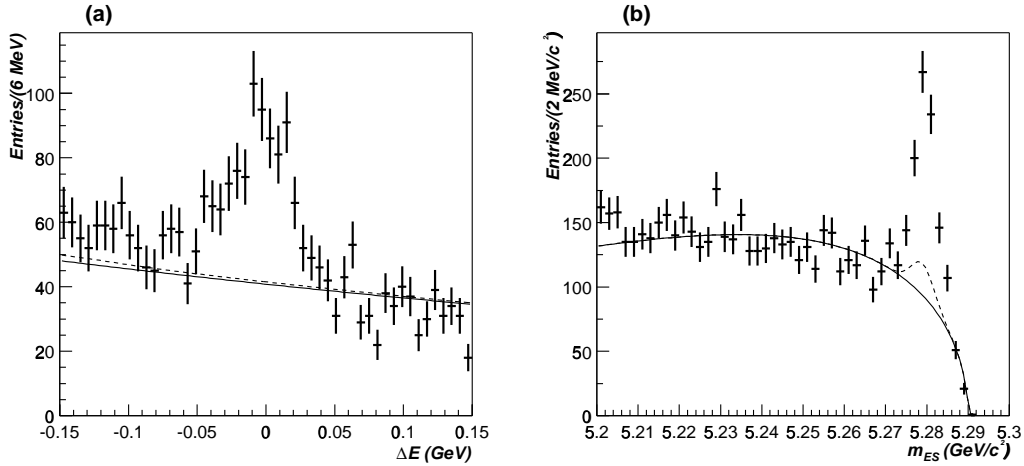
Figure 2: On-resonance signal region ΔE (a) and m_{ES} (b) distributions for $B^{\pm} \rightarrow \pi^{\pm}\pi^{\mp}\pi^{\pm}$. The solid lines show the expected level of continuum background, using appropriately normalised background shapes from the sideband regions in on-resonance data. The dotted lines show the expected level of $B\overline{B}$ background, which is obtained from the sum of Gaussian distributions from Monte Carlo estimated cross-feed and $D^0\pi$ events, each normalised to the number of events observed in on-resonance data that passed the selection criteria for $B^{\pm} \rightarrow \pi^{\pm}\pi^{\mp}\pi^{\pm}$.

Figure 3: On-resonance signal region ΔE (a) and m_{ES} (b) distributions for $B^{\pm} \rightarrow K^{\pm}\pi^{\mp}\pi^{\pm}$.
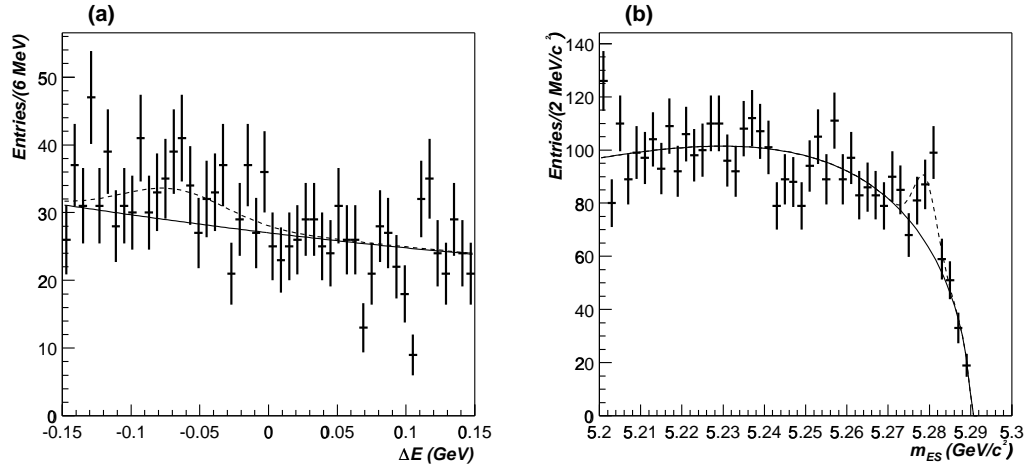
138

Figure 4: On-resonance signal region ΔE (a) and m_{ES} (b) distributions for $B^{\pm} \to K^{\pm}K^{\mp}\pi^{\pm}$.
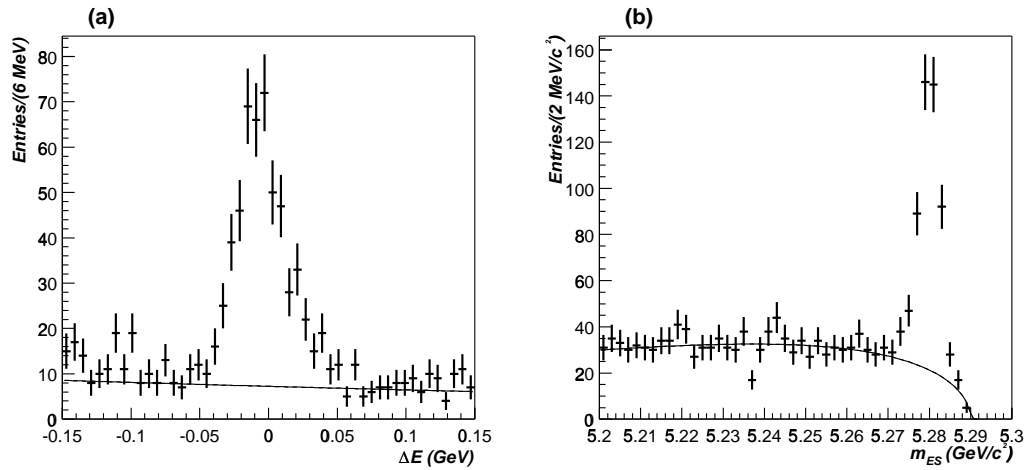

Figure 5: On-resonance signal region ΔE (a) and m_{ES} (b) distributions for $B^{\pm} \to K^{\pm}K^{\mp}K^{\pm}$.
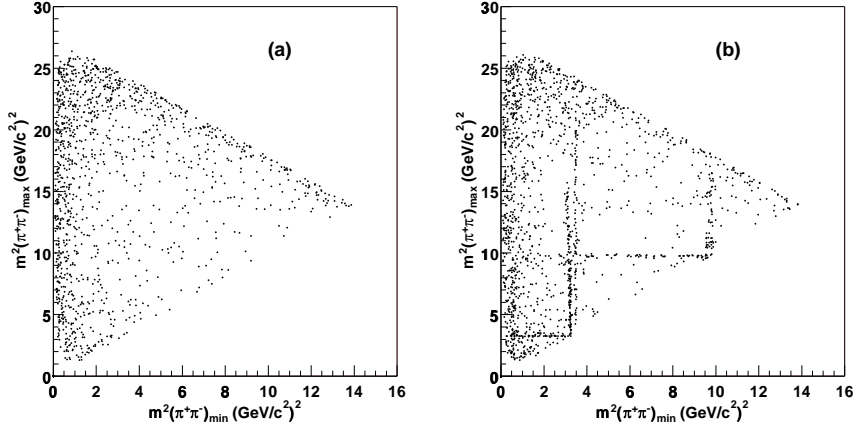
Figure 6: Unbinned Dalitz plots for on-resonance data for $B^{\pm} \to \pi^{\pm}\pi^{\mp}\pi^{\pm}$ for GSB region (a) and signal region (b). No efficiency corrections have been applied, and the open charm contributions are included in the plots.
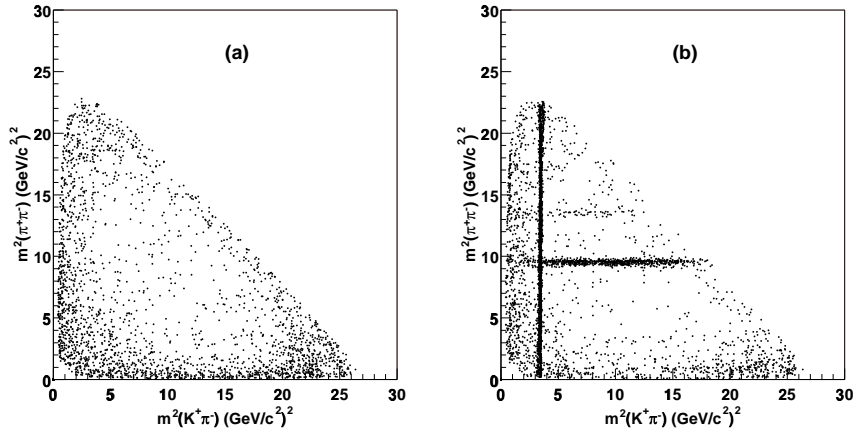

Figure 7: Unbinned Dalitz plots for on-resonance data for $B^{\pm} \to K^{\pm}\pi^{\mp}\pi^{\pm}$ for GSB region (a) and signal region (b).

The preliminary results are: $Br(\pi^{\pm}\pi^{\mp}\pi^{\pm}) < 15 \times 10^{-6}$, $Br(K^{\pm}\pi^{\mp}\pi^{\pm}) = (59.2 \pm 4.7 \pm 4.9) \times 10^{-6}$, $Br(K^{\pm}K^{\mp}\pi^{\pm}) < 7 \times 10^{-6}$, and $Br(K^{\pm}K^{\mp}K^{\pm}) = (34.7 \pm 2.0 \pm 1.8) \times 10^{-6}$.
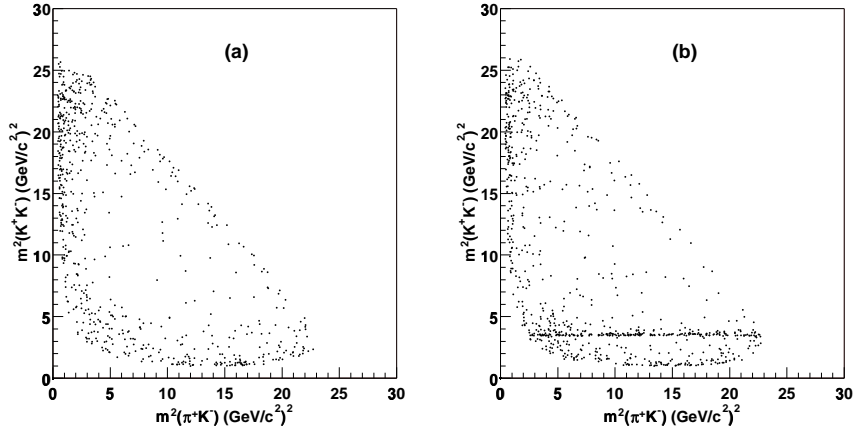
Figure 8: Unbinned Dalitz plots for on-resonance data for $B^{\pm} \to K^{\pm}K^{\mp}\pi^{\pm}$ for GSB region (a) and signal region (b).

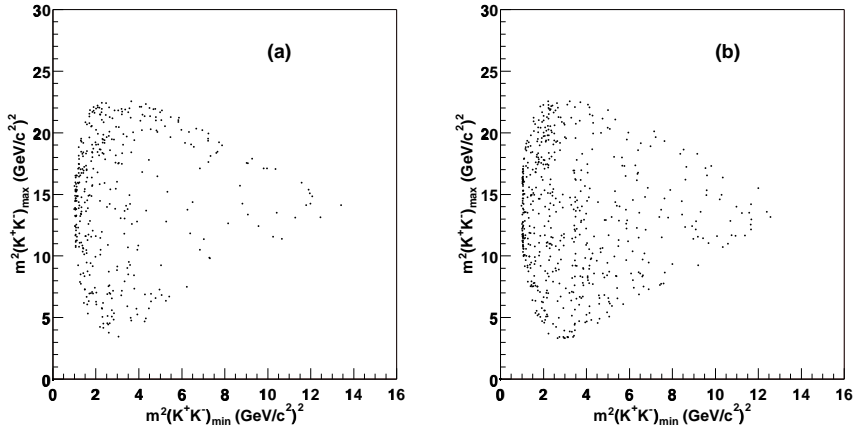Figure 9: Unbinned Dalitz plots for on-resonance data for $B^{\pm} \to K^{\pm}K^{\mp}K^{\pm}$ for GSB region (a) and signal region (b).

References

[1] Charmless hadronic B decays at BABAR, Marcella Bona (for the BABAR Collaboration) submitted to EPS HEP 2001, hep-ex/0111017

[2] A. Ali, G. Kramer, and C. D. Lü, Phys. Rev. D **58**, 094009 (1998); Y. H. Chen

et al., Phys. Rev. D **60**, 094014 (1999).

[3] CLEO Collaboration (S. J. Richichi *et al.*) Phys. Rev. Lett. **85**, 520 (2000); CLEO CONF 99-12 (1999).

[4] M. Gronau and J. L. Rosner, Phys. Rev. D **53**, 2516 (1996); A. S. Dighe, M. Gronau, and J. L. Rosner, Phys. Rev. Lett. **79**, 4333 (1997); M. R. Ahmady, E. Kou, and A. Sugamoto, Phys. Rev. D **58**, 014015 (1998); D. Du, C. S. Kim, and Y. Yang, Phys. Lett. **B426**, 133 (1998).

[5] H. J. Lipkin, Phys. Lett. B **254**, 247 (1991).

[6] CLEO Collaboration, D. M. Asner *et al.*, "Search for Exclusive Charmless Hadronic B Decays", Phys. Rev. D **53**, 1039 (1996), hep-ex/9508004.

[7] Particle Data Group, D. E. Groom *et al.*, Eur. Phys. Jour. C **15**, 1 (2000).

[8] I. Halperin and A. Zhitnitsky, Phys. Rev. D **56**, 7247 (1997); E. V. Shuryak and A. Zhitnitsky, *ibid.* **57**, 2001 (1998).